

1

2

3 (Original Research)

4

5 **Mechanistic insights into the structure-dependant and strain-specific utilization of**  
6 **wheat arabinoxylan by *Bifidobacterium longum***

7 Ang-Xin Song <sup>a</sup>, Long-Qing Li <sup>a</sup>, Jun-Yi Yin <sup>b</sup>, Jia-Chi Chiou <sup>a,\*</sup>, Jian-Yong Wu <sup>a,\*</sup>

8 <sup>a</sup> Food Safety and Technology Research Center, Department of Applied Biology & Chemical  
9 Technology, The Hong Kong Polytechnic University, Hung Hom, Kowloon, Hong Kong

10 <sup>b</sup> State Key Laboratory of Food Science and Technology, Nanchang University, Nanchang,  
11 Jiangxi 330047, China

12

13 \* *Corresponding authors:*

14 Tel: +852 3400 8671; fax: +852 2364 9932.

15 E-mails: [jian-yong.wu@polyu.edu.hk](mailto:jian-yong.wu@polyu.edu.hk) (J.Y. Wu); [jiachi.amber.chiou@polyu.edu.hk](mailto:jiachi.amber.chiou@polyu.edu.hk) (JCC)

## 16    **Abstract**

17    Arabinoxylan (AX), an important dietary fiber from cereal grains, is mainly metabolised in the  
18    large intestine by gut bacteria, especially bifidobacteria. This study investigated the uptake and  
19    metabolism of wheat AX by a *Bifidobacterium longum* strain that could grow well with AX as  
20    the sole carbon source. The bacterial growth rate showed a significant correlation to the  
21    molecular weight (MW) of AX and its acid hydrolysates. Assessment of the key AX degrading  
22    enzymes suggested that the uptake and consumption of AX involved extracellular cleavage of  
23    xylan backbone and intracellular degradation of both the backbone and the arabinose  
24    substitution. The preference for native or partially hydrolysed AX with single substitutions and  
25    a sufficiently high MW suggested the structure-dependant uptake by the bacterial cells. Genetic  
26    analysis of *B. longum* showed the lack of  $\beta$ -xylosidase, suggesting the existence of unknown  
27    enzymes or dual/multiple-specific enzymes for hydrolysis of the non-reducing end of xylan  
28    backbone.

29

30    *Keywords:* *Bifidobacteria*; Arabinoxylan; Molecular weight; Degradation mechanism; Strain-  
31    specific; Structure-dependence; Genomic analysis

32

## 33    **1. Introduction**

34       The human gastrointestinal tract (GIT) is inhabited by a highly diverse microbial  
35    community referred to as gut microbes which are essentially important for its functions on the  
36    human health (Eckburg et al., 2005). Until now this densely populated ecosystem remains  
37    incompletely characterized as over 20% of the identified microbiota species cannot be cultured

38 artificially (Lagier et al., 2016). Five bacterial phyla have been revealed to dominate the human  
39 GIT microbiota with *Firmicute* being the most abundant followed by *Bacteroides*,  
40 *Actinobacteria*, *Proteobacteria* and *Verrucomicrobia* (Tap et al., 2009). The *Bifidobacterium*  
41 genus belonging to gut *Actinobacteria* is one of the prevalent groups of culturable anaerobic  
42 bacteria within mammalian GIT (Pokusaeva, Fitzgerald, & van Sinderen, 2011) and among the  
43 first colonizers in human GIT (Favier, Vaughan, De Vos, & Akkermans, 2002). Although  
44 bifidobacteria compose only 3-6% of the adult fecal flora, their presence is thought to  
45 contribute to various health benefits, such as prevention of pathogen colonization,  
46 improvement of lactose intolerance and modulation of the immune response (Rastall et al.,  
47 2005; Schell et al., 2002). Because of their health promoting effects, certain bifidobacterial  
48 strains are commercially exploited as functional food ingredients (Pokusaeva et al., 2011).  
49 Several of the health promoting activities of bifidobacteria as well as their adaptation to the  
50 human GIT are associated with their ability to utilize various carbohydrates that are non-  
51 digestible in the human GIT. Therefore, understanding the carbohydrate utilization by  
52 bifidobacteria may help to reveal the mechanisms of beneficial interactions in the human GIT.

53       Arabinoxylan (AX) is the main non-starch polysaccharide found in cereal grains, such as  
54 wheat, rye, rice, barley and oats. It consists of a linear  $\beta$ -1,4-linked xylose backbone which can  
55 be randomly substituted at the C(O)2 and/or C(O)3 positions with arabinose monomers  
56 (Izydorczyk & Biliaderis, 1995). AX and AX oligosaccharide (AXOS) cannot be digested by  
57 human enzymes in the GIT and can directly enter the colon, providing the energy sources for  
58 certain saccharolytic organisms (Rivière et al., 2014). Currently, *Bacteroides* and *Roseburia*  
59 are the only known gut xylanolytic taxa that are able to hydrolyze the backbone of AX by

60 producing extracellular endo-xylanases (Chassard, Goumy, Leclerc, Del'homme, & Bernalier-  
61 Donadille, 2007; Leth et al., 2018). However, many bifidobacterial strains are able to utilize  
62 AX, AXOS or XOS. The bifidogenic effect of AX also indirectly affects some other genera in  
63 human GIT probably through cross-feeding (Falony, Vlachou, Verbrugghe, & Vuyst, 2006;  
64 Van den Abbeele, Gérard, Rabot, Bruneau, El Aidy, Derrien, Kleerebezem, Zoetendal, Smidt,  
65 Verstraete, et al., 2011).

66 Although several studies have demonstrated the utilization of AX by bifidobacteria, the  
67 degradation mechanism is still unclear. Many of these studies have been mainly concerned  
68 with the bifidogenic effects of AX or AXOS by assessing the bacterial growth, pH change and  
69 short-chain fatty acid production (Crittenden et al., 2002; Van Laere, Hartemink, Bosveld,  
70 Schols, & Voragen, 2000). In addition, most previous studies have considered the gut  
71 bifidobacteria as a whole (Neyrinck et al., 2011) but few have specifically investigated the  
72 influence of AX molecular structure on its utilization by the bifidobacterial cells. A recent  
73 study based on 36 bifidobacterial strains has indicated that the AX degradation process is  
74 strain-dependent (Rivière et al., 2014). Besides, it was the fine structure of AX rather than the  
75 general structure that mainly governed its fermentation (Mendis, Leclerc, & Simsek, 2016).  
76 Therefore, investigation of the AX metabolism process of individual bifidobacterial strains is  
77 of great importance for understanding the mechanisms adopted by the whole gut bifidobacterial  
78 population and the dynamic effects of different non-digestible carbohydrates on the intestinal  
79 microbiota populations. This study was to investigate the wheat AX degradation process by  
80 *Bifidobacterium longum* CICC6186. The genome sequence of this strain was determined and  
81 analysed to determine the correlations with its metabolic mechanisms on AX.

82

## 83 **2 Materials and Methods**

### 84 **2.1. Chemicals and enzymes**

85 Wheat AX (P-WAXYH) was purchased from Megazyme (~95% purity, > 40 cSt viscosity,  
86 arabinose: xylose (%) = 38:62). Arabinose (1001925) was from International Laboratory USA  
87 and xylose (14100) from Acros Organics (USA). Galacto-oligosaccharides (GOS) were  
88 purchased from New Francisco Biotechnology Co., Ltd. (China) and xylo-oligosaccharides  
89 (XOS) from Shandong Longli Biotechnology CO., Ltd (China). The molecular weights (MW)  
90 of AX, GOS and XOS were determined before use (Figure S1 & Table 1).

91 The  $\alpha$ -L-arabinofuranosidase (E-ABFUM, GH62) originated from *Ustilago maydis* and  
92  $\alpha$ -L-arabinofuranosidase (E-ABFBO17, GH43) originated from *Bacteroides ovatus* were  
93 purchased from Megazyme (Ireland).

94

### 95 **2.2 Preparation and analysis of AX samples**

#### 96 **2.2.1 Degradation and de-branching of AX**

97 The native AX from the supplier was partially hydrolysed to lower MW fractions by  
98 trifluoroacetic acid (TFA) under well controlled. In brief, 0.25 g of AX was mixed with 20 mL  
99 of 0.1 M TFA in a 100 mL round bottom flask at 90 °C with vigorous stirring for 10, 30 or 60  
100 min, yielding AX-10, AX-30 or AX-60. The residual TFA was removed by evaporation in  
101 vacuum at 40 °C with a rotary evaporator and the solid residual was washed several times with  
102 methanol, and then re-dissolved in 10 mL water. The solution was freeze-dried to give the acid-  
103 hydrolysed AX fractions.

The  $\alpha$ -L-arabinofuranosidase (E-ABFUM, specifically cleaving non-reducing  $\alpha$ -L-arabinofuranose from singly substituted xylose residues in AX) and  $\alpha$ -L-arabinofuranosidase (E-ABFBO17, specifically hydrolysing  $\alpha$ -1, 3-arabinofuranose from double substitution) were applied for the de-branching of AX separately. AX (5 mg/mL) in sodium phosphate buffer (100 mM, pH 6.5) or sodium acetate buffer (100 mM, pH 5.0) was mixed with  $\alpha$ -L-arabinofuranose from *Bacteroides ovatus* or *Ustilago maydis*, respectively, and then incubated at 40 °C for 30 min with stirring. Enzyme was denatured by boiling for 10 min. De-branched AX was then freeze dried.

### 2.2.2 Molecular weight analysis of AX and hydrolysates

The native AX was treated by ultrasound as described by Chen et al (2014) to lower its viscosity. The MW of native and acid-hydrolysed AX was determined by high-pressure gel permeation chromatography (HPGPC) as reported previously (Song, Mao, Siu, & Wu, 2018). Briefly, samples were dissolved in Milli-Q water (0.5-1 mg/mL), centrifuged at 6000 rpm for 15 min and filtered through 0.45  $\mu$ M membrane before injection. A Waters 1515 isocratic pump system equipped with a 2414 refractive index detector and three columns in series, Ultrahydrogel 120, 250 and 2000 (Waters Co., Milford, MA, USA) at 50 °C was applied for the MW analysis. The flow rate of mobile phase (Milli-Q water) was fixed at 0.6 mL/min. Dextran MW standards of nine different MWs in the range of 1.0-670 kDa (Sigma-Aldrich) were applied to obtain the calibration curve.

### 2.2.3 $^1\text{H}$ NMR of de-branched AX

Before the  $^1\text{H}$  NMR analysis, de-branched samples were dissolved in deuterium oxide (10 mg/mL) and then lyophilized (Rose, Patterson, & Hamaker, 2009). Both the dissolution and lyophilization steps were repeated twice and the samples were re-dissolved in deuterium oxide. The  $^1\text{H}$  NMR analysis was performed on a Bruker Avance-III 400 MHz FT-NMR system.

## 2.3 Bacterial strains and culture conditions

Five *Bifidobacterial* strains from China Centre of Industrial Culture Collection (CICC) were used in this study including *B. adolescentis* CICC6070, *B. bifidum* CICC10395, *B. breve* CICC6079, *B. infantis* CICC6069 and *B. longum* CICC6186 (JCM 1217), which were stocked and incubated under the conditions as described previously (Song et al., 2018). Experiments in this study were all performed in liquid culture on Reinforced Clostridial Medium (RCM) broth. Prior to the liquid culture, the bacteria taken from the stock (30% glycerol at -80 °C) were inoculated on RCM agar and incubated for about 2 days. A single colony was picked from the solid culture and inoculated into 5 mL of RCM broth and then incubated for about 24 h at 200 rpm to be used as the starter culture for the experimental cultures. The bacterial cultures were all incubated at 37 °C under anaerobic condition in air-tight jars with anaerobic sachets (AnaeroGen TM, Thermo Scientific Oxoid, USA).

Initial experiments were performed with five strains of bifidobacteria cultured with the native AX as the sole carbon source. The AX was added at 5 g/L final concentration to a glucose-free RCM broth (5 mL), which was dispensed in 10 mL centrifuge (culture) tubes. Glucose as the standard carbon source in the normal culture medium and GOS as a prebiotic reference were included for comparison and glucose-free RCM broth was used as the control

group. All liquid media were sterilized by autoclaving at 121 °C for 20 min before use. The culture experiments were then initiated by inoculation of bacterial suspension from the starter culture into the liquid medium at 2% (v/v) and incubation on a shaker at 200 rpm for 24 h. The optical density (OD) which is proportional to the bacterial density was measured at 600 nm with a spectrophotometer. As *B. longum* was found to be the only strain that was able to grow well on AX, it was mainly used in the later experiments. XOS, arabinose, xylose and the mixture of arabinose and xylose at 1:2 molar ratio (total concentration 5 g/L) were applied as the single carbon sources for the growth of *B. longum*.

## **2.4 Analysis of AX degrading enzymes**

### **2.4.1 Preparation of bacterial enzymes**

AX was applied at 5 g/L to the bacterial culture as the carbon source in comparison with the normal carbon source glucose (5 g/L). *B. longum* was cultivated for 16 h to accumulate sufficient amount of active enzymes according to the growth curve. Parallel experiments were performed with *B. infantis* as comparison which could not use AX for growth. About 0.3 g wet mass of the bacterial cells was recovered from the bacterial culture broth by centrifugation at 4000 rpm for 8 min, washed twice by phosphate buffer (100 mM NaH<sub>2</sub>PO<sub>4</sub>, 0.02% w/v NaN<sub>3</sub>, pH6.0), and re-suspended in 30 mL of phosphate buffer. The cell suspension was homogenized at 4 °C with a French Press at  $1.38 \times 10^5$  kPa for three cycles (Derensy-Dron, Krzewinski, Brassart, & Bouquelet, 1999). The cell extract liquid was separated from the cell debris by centrifugation at 10,000 rpm for 30 min. The cell extract as well as the culture medium was stored at -80 °C before the enzyme analysis.



#### 2.4.2 Determination of enzyme activity on standard substrates

The  $\beta$ -xylosidase and  $\alpha$ -L-arabinosidase activities in the bacterial extract and culture medium were determined with a slightly modified procedure as reported by Zeng et al. (2007). The *p*-nitrophenyl- $\beta$ -D-xyloside (*p*NPX) (S31323, Shanghai Yuanye Biotechnology Co., Ltd, China) and *p*-nitrophenyl- $\alpha$ -L-arabinofuranoside (*p*NPA) (O-PNPAF, Megazyme) were applied as the substrates for  $\beta$ -xylosidase and  $\alpha$ -L-arabinosidase, respectively. One activity unit was defined as the amount of enzyme that produced 1  $\mu$ mol of *p*-nitrophenol per min at 40 °C. The reaction mixture containing 100  $\mu$ L of 10 mM of substrates in a phosphate buffer (100 mM NaH<sub>2</sub>PO<sub>4</sub>, 0.02% w/v NaN<sub>3</sub>, pH6.0) and 100  $\mu$ L of crude enzymes were incubated at 40 °C for 10 min. The reaction was stopped by addition of 0.6 mL of 1 M Na<sub>2</sub>CO<sub>3</sub>, and the optical density was measured at 405 nm using *p*-nitrophenol as a standard.

A xylanase assay kit (K-XyIX6-1V, Megazyme) was used for determination of the endo-xylanase activity. In brief, XyIX6 substrate reagent was mixed with properly diluted crude enzymes and incubated at 40 °C for 10 min. Tris buffer (2% w/v, pH 10.0) was added to stop the reaction and the absorbance was measured at 400 nm. One activity unit was defined as the amount of enzyme required to release 1  $\mu$ mol of *p*-nitrophenol from XyXI6 substrate in one minute.

#### 2.4.3 Determination of enzyme activity on AX degradation

Since  $\beta$ -xylosidase and  $\alpha$ -L-arabinosidase activities were not detected in the culture medium, only the cell extract was tested for AX degrading activity. The cell extract at 0.4 mL

was mixed with 1.6 mL of AX solution (5 g/L), and incubated at 37 °C and 200 rpm on a shaker for 24 h. The monosaccharides produced in the reaction mixture were determined by 1-phenyl-3-methyl-5-pyrazolone (PMP)-high-performance liquid chromatograph (HPLC) method (Song et al., 2018). For the HPLC analysis, the reaction mixture (450 µL) was added 450 µL of 0.5 M PMP in methanol and 450 µL of 0.3 M NaOH and then stirred at 70 °C for 30 min. The reaction was stopped by adding 450 µL of 0.3 M HCl and washed thrice with chloroform. The aqueous layer was collected and filtered through a 0.45 µM membrane before injection. The HPLC was performed with an Agilent Eclipse XDB-C18 column (4.6 × 250 mm) at 25 °C and UV detector at 250 nm. Potassium phosphate buffer (0.05 M, pH 6.9) with 15% (A) and 40% (B) acetonitrile was used as the mobile phase. The peaks were identified and quantified with glucose, arabinose and xylose standards. To eliminate errors from cell extract itself, mixture of cell extract and deionized (DI) water was tested as the blank.

## **2.5 Analysis of AX degradation products**

For quantifying the degradation of AX by *B. longum*, AX was applied as the sole carbon source. Soluble starch was excluded from the culture medium only when acid hydrolysis was applied to determine the concentration and monosaccharide composition of AX. The *B. longum* bacteria were cultured for 24 h and then centrifuged at 4000 rpm for 8 min for collection of the supernatant. The bacterial cell extract was prepared with the same procedure as described in 2.4.1.

The MW profile of culture medium was determined by high-pressure gel permeation chromatography (HPGPC) as described in 2.2.2. Monosaccharides in the culture medium and cell extract were determined by the PMP-HPLC method as described in 2.4.3.

The concentration and monosaccharide composition of AX in the culture medium and cell extract were determined by analysis of neutral sugars following acid hydrolysis. The culture medium or cell extract sample (1.7 mL) was mixed with 0.3 mL of TFA to attain 2 M TFA final concentration. The mixture was stirred at 110 °C for 4 h, followed by vacuum evaporation to dryness. The solid residual was washed several times by methanol and re-dissolved in 1.7 mL water for monosaccharide analysis by PMP-HPLC.

The change of AX side chains in the culture medium during fermentation (0, 4, 8, 12, 16, 20, 24 h) was monitored by <sup>1</sup>H NMR. The culture medium was collected and centrifuged to remove the bacteria, and then lyophilized and dissolved in deuterium oxide. The solution and lyophilisation steps were repeated twice and the samples were re-dissolved in deuterium oxide before <sup>1</sup>H NMR analysis.

## **2.6 Genome sequencing and analysis**

The genome of *B. longum* was sequenced using an Illumina HiSeq 4000 system (Illumina, San Diego, CA, USA) at Beijing Genomics Institute (Shenzhen, China) and the genome analysis was done by Shanghai Majorbio Bio-pharm Technology Co., Ltd. (Shanghai, China). Raw reads of low quality from paired-end sequencing (those with consecutive bases covered by fewer than five reads) were discarded. The sequenced reads were assembled using SOAPdenovo (v2.04) (<http://soap.genomics.org.cn/>). Glimmer (v 3.02) and GeneMarks (v 4.3)

were run to model the coding sequence (CDS) of the gene. Predicted amino acid sequences of CDS were searched against COG, KEGG and CAZy database by BLAST+ and Diamond, and whenever possible, proteins were also predicted based on these database. The rRNA and tRNA were identified using Barrnap and tRNA-scan-SE, respectively.

### **3. Results and discussion**

#### **3.1 Molecular weight profiles of AX and its acid-hydrolysates**

Probiotic bacteria can selectively utilize different carbohydrate sources based on their monosaccharide composition and structure characteristics, such as degree of polymerization (DP), linkage types and branch chains. For a given carbohydrate polymer, DP is a major factor for bacterial utilization and a lower DP is usual more favourable for bacterial consumption and growth. Molecular weight (MW) which is directly correlated to DP is also an important characteristic of the carbohydrate substrate for probiotic bacteria.

As shown in Table 1 and Figure S1 (supplemental data), the native AX exhibited a single peak on the GPC corresponding to an average MW of 359,829. All the AX acid hydrolysates exhibited two peaks, the higher MW peaks showed a dramatic decrease with the hydrolysis time and the lower MW peaks were about 172-176.

Polysaccharide branches are usually more susceptible than their backbones to TFA hydrolysis (Mori, Eda, & Kato, 1979; Wang, Zhao, Song, Song, Fu, & Zhang, 2015). The monosaccharide content in AX hydrolysate showed a sharp increase from 0 to 38.9% in the first 10 min, a smaller increase in the following 20 min to 53.3%, and little or no increase in the last 30 min. This was due most probably to the relatively easy hydrolysis of arabinose

branches which accounted for ~33% of AX mass (Table 5). After most of the branches had been degraded, it was difficult to cleave the free xylose from the backbone. A similar procedure was applied by Mori et al (1979) to cleave arabinose branches on arabinoxyloglucan for production of xyloglucan. Table 1 also shows the MW of two oligosaccharide references, GOS with degree of polymerization ~3-6 and XOS ~2-5.

Table 1 Molecular weight distributions of AX samples and OS references derived from GPC analysis.

	Retention time (min)	MW (Da)	Area %
AX	38.517	359,829	100.00
AX-10	41.750	39,499	61.06
	51.743	176	38.94
AX-30	45.350	8,650	46.66
	51.742	176	53.34
AX-60	46.850	1,661	50.18
	51.759	172	49.82
GOS	48.791	841	53.79
	49.490	409	44.27
XOS	49.267	747	59.78
	50.236	290	40.22

### 3.2 Bacterial growth

Table 2 shows the relative growth rates of five bifidobacterial strains on various carbon sources. All the five strains of bifidobacteria grew well on GOS, which was in agreement with the results reported previously (Kondepudi, Ambalam, Nilsson, Wadström, & Ljungh, 2012).

Moderate growth of *B. breve* and *B. bifidum* was observed on glucose. *B. breve* could also grow weakly even in the absence of a carbon source, suggesting its ability to obtain carbon nutrients from other medium ingredients. *B. longum* was the only strain which could grow well on AX at a growth rate even higher than on glucose or GOS. Although the ability of *B. longum* to grow on AX and AX oligosaccharide (AXOS) has been reported previously (Crittenden et al., 2002), it is a new and interesting finding that this bacterium grew much more actively on AX than on glucose or the low-MW GOS. As the only strain capable of utilizing AX, *B. longum* was mainly used in the following experiments.

Table 2 Growth of five bifidobacterial strains on different carbon sources.

Bacteria	Control	Glc	GOS	AX
<i>B. adolescentis</i>	-	++	++	-
<i>B. breve</i>	+	+	++	+
<i>B. bifidum</i>	-	+	++	-
<i>B. infantis</i>	-	++	++	-
<i>B. longum</i>	-	++	++	+++

Scale: OD < 0.1 (- = no growth), 0.1-0.49 (+ = mild growth), 0.5-0.89 (++ = moderate growth), > 0.9 (+++ = strong growth).

As shown by the growth curves of *B. longum* (Figure 1A), the bacterial growth on glucose turned from an initial lag period to the exponential phase at ~ 7 h. The growth on AX stayed in a lag period with negligible growth until ~ 8 h and then experienced a slow growth period between 8-12 h, and entered the exponential phase at 12-13 h. On AX, the exponential growth period was much shorter (from 12-15 h) but the rate was higher than on glucose. The long

period of lag and slow growth of the bacteria on AX could be explained by that the large AX molecules need to be degraded by enzymes from the bacteria before being utilized. In the early period of culture when the bacterial concentration was very low, there were few enzymes available to degrade AX for the bacterial growth. After the lag period, the bacterial concentration increased gradually and the rate of AX degradation increased, so that the bacterial growth was significantly enhanced. The much more rapid growth of the bacteria on AX during the exponential suggested that the degraded AX was a more favourable carbon source than glucose for the bacterial growth. The growth of bacteria cultured on AX-10, AX-30 and AX-60 had a very short lag period of no more than 5 h, which was probably mostly due to the consumption of arabinose contained the AX hydrolysates. Crittenden et al (2002) showed the quick start of growth of two different bifidobacterial strains on arabinose in about 4 h. The growth of *B. longum* on AX-10 (11-13 h), AX-30 (10-13 h) and AX-60 (9-12 h) entered the exponential growth phase earlier than on AX. This suggests that the acid-degraded AX were more readily utilized by the bacteria for growth than the larger and native AX.

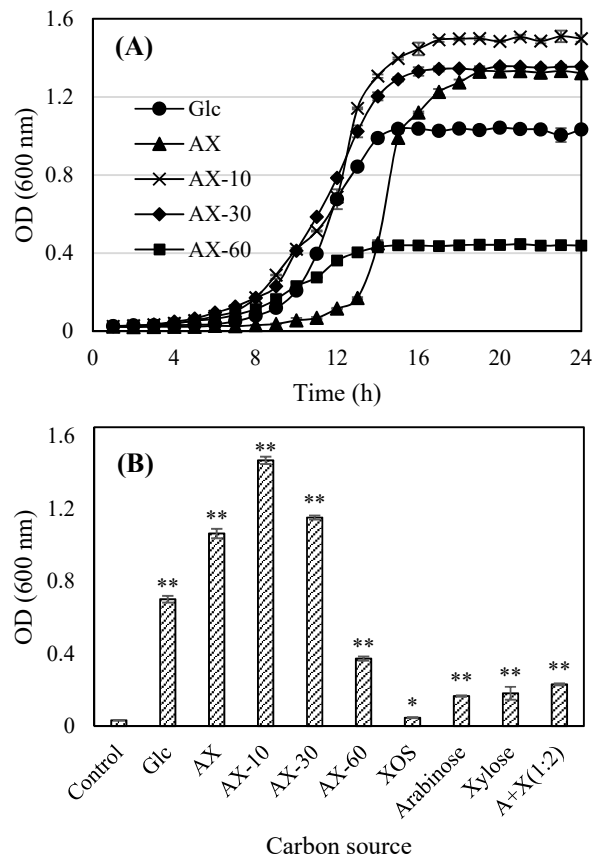


Figure 1 (A) Growth curve of *B. longum* on glucose and arabinoxyylan (AX), and (B) Growth of *B. longum* on different carbon sources (AX-10, 30, 60: acid hydrolysis for 10, 30, 60 min; A+X (1:2): arabinose and xylose at molar ration of 1:2; \*: P < 0.05, \*\*: P < 0.01 by *t*-test for the statistically significant difference from control).

It is very unusual and noteworthy that AX could be effectively fermented and utilized by a single *B. longum* bacterium in a pure culture. Although the native AX increased the growth of bifidobacteria similarly to AXOS in animal models (Geraylou et al., 2012; Neyrinck et al., 2011; Van den Abbeele, et al., 2011), the abundance of bifidobacterial population (bifidogenic effect) in fecal cultures was only increased with the oligosaccharides including AXOS or XOS (Rycroft, Jones, Gibson, & Rastall, 2001; Vardakou, Palop, Gasson, Narbad, &



Christakopoulos, 2007) but not with the long chain AX (Hopkins et al., 2003). In pure cultures of certain bifidobacterial strains, XOS and AXOS were more effectively utilized than AX for the bacterial growth (Jaskari et al., 1998; Pastell, Westermann, Meyer, Tuomainen, & Tenkanen, 2009). These studies generally suggest that AX is less fermentable than AXOS or XOS by most bifidobacterial strains. The different utilization rates of AX in the bifidobacterial cultures suggests that the metabolic activity of bifidobacteria on the native and partially hydrolysed AX was species- or strain-dependant.

Figure 1B shows the OD values of *B. longum* after 24 h of growth on various carbon sources. First of all, the bacterial growth on the native AX was notably higher than on glucose (OD 1.06 versus OD 0.70) and was further increased with AX-10 by nearly 40% (OD 1.47). However, the growth dropped from the highest OD with AX-10 to OD1.15 with AX-30, and even lower OD of 0.37 with AX-60. More surprisingly, the *B. longum* bacteria showed a poor growth on the two monosaccharide constitutes of AX, arabinose, xylose and their mixture, and barely any growth on XOS (MW ~300-750).

Overall, AX (MW~359,829) and its moderately hydrolysed products with a relatively high MW including AX-10 (MW~39,499) and AX-30 (MW ~8650) were much more favourable for the *B. longum* growth than the low-MW hydrolysate AX-60 (MW ~1661) and the constituent monosaccharides of AX. Similarly, a previous study on fish showed that AXOS with a higher degree of polymerization (DP) had a stronger stimulating effect on the growth of lactic acid bacteria than the AXOS of a lower DP (Geraylou et al., 2012). In another study, some bifidobacterial strain showed a selectivity on the content of arabinose side chains in AXOS and a better growth on AXOS with a higher content of arabinose substitution along the XOS

backbone (Jaskari et al., 1998). These results from the present and previous studies suggest that the specific side-chain structure in AX or AXOS could be recognized by the bifidobacterial cell and selectively metabolized. In the present study, when the acid hydrolysis of AX was very extensive and destructive of the side-chains, the hydrolysed low-MW products such as AX-60 could not be well utilized by the *B. longum* cell.

### 3.3 Activities of AX degrading enzymes

Table 3 shows the major enzymes involved in AX degradation in *B. longum* and *B. infantis* cells and culture medium. Only endo-xylanase was detected in the culture medium of both bacterial strains and the other two enzymes,  $\alpha$ -L-arabinosidase and  $\beta$ -xylosidase were detected in the cells of both bacterial strains. Endo-xylanase was detected only in the *B. longum* cells but not in *B. infantis* cells. The activities of endo-xylanase and  $\alpha$ -L-arabinosidase from the *B. longum* were notably higher in the culture with AX than with glucose as the carbon source. Although the possible release of extracellular  $\alpha$ -L-arabinofuranosidases by some bifidobacterial strains has been reported, no such enzymes from the *B. longum* have been documented (Schell et al., 2002; van den Broek, Hinz, Beldman, Vincken, & Voragen, 2008). Although *B. infantis* did not utilize AX, it exhibited higher activities of  $\alpha$ -L-arabinosidase and  $\beta$ -xylosidase enzymes than *B. longum*. Two arabinofuranohydrolases (AXH-d3 and AXH-m23) in *B. adolescentis* DSM 20083 have been found active only on AX (Van Laere et al., 1999), while a GH family 43 arabinofuranosidase (Abf3) in *Lactobacillus brevis* DSM 20054 displayed a highly specific activity for arabinobiose but could not release arabinose from AXOS (Michlmayr et al., 2013). In a word, this was mainly attributed to the substrate

specificity of enzymes. In the present study, the enzymes detected in *B. infantis* were probably specific and active to some other carbohydrates such as araban and arabinogalactan but not to AX. The results in Table 4 proved that  $\alpha$ -L-arabinosidase and  $\beta$ -xylosidase produced by *B. infantis* had barely any activity on AX.

Table 3 Activities of AX degrading enzymes in culture medium and cell extract (U/mL).

	Carbon source	Endo-xylanase	$\alpha$ -L-Arabinosidase	$\beta$ -xylosidase
<i>B. longum</i>				
Medium	Glc	0.013 $\pm$ 0.004	-	-
	AX	<b>0.044 <math>\pm</math> 0.013</b>	-	-
Cell extract	Glc	0.005 $\pm$ 0.002	0.017 $\pm$ 0.003	0.0133 $\pm$ 0.003
	AX	<b>0.017 <math>\pm</math> 0.002</b>	<b>0.032 <math>\pm</math> 0.004</b>	0.0130 $\pm$ 0.001
<i>B. infantis</i>				
Medium	Glc	0.028 $\pm$ 0.004	-	-
	AX	0.027 $\pm$ 0.002	-	-
Cell extract	Glc	-	0.065 $\pm$ 0.004	0.287 $\pm$ 0.017
	AX	-	0.059 $\pm$ 0.002	0.273 $\pm$ 0.014

With glucose or AX as the carbon source, only trace amount of arabinose was detected through the enzymatic hydrolysis of AX by cell extract of *B. infantis* (Table 4). This suggests that the  $\alpha$ -L-arabinosidase and  $\beta$ -xylosidase in *B. infantis* cell could not be induced by AX. On the other hand, the enzymes in *B. longum* cell were activated by AX to cleave the arabinose and xylose residues in AX, which suggests the intracellular degradation of AX by this bacterial strain. Only when AX was applied, could the enzymes in *B. longum* be activated to cleave the backbone of AX into monosaccharides, though the amount of xylose produced was critical. Similar results have been reported by Lagaert et al. (2011), showing that two  $\beta$ -xylosidases in

*B. adolescentis* could only hydrolyse xylose from XOS but had low activity on AX. This observation suggests that the  $\beta$ -xylosidases could only hydrolyse the non-reducing end of the xylan backbone until they are stopped by substituted residues. Therefore,  $\beta$ -xylosidases had little activity on AX to produce xylose. The induced activities of  $\alpha$ -L-arabinofuranosidase and  $\beta$ -xylosidases inside *B. longum*, as well as the production of xylose and arabinose from AX hydrolysis by the *B. longum* cell extract, indicates intracellular degradation of AX or AXOS by *B. longum*.

Table 4 Monosaccharides produced through enzyme hydrolysis of AX by bacterial cell extract.

Carbon source	Monosaccharide	Concentration (g/L)
<i>B. longum</i>		
AX	xylose	$(1.41 \pm 0.51) \times 10^{-3}$
	arabinose	$0.21 \pm 0.03$
Glc	xylose	-
	arabinose	$(0.19 \pm 0.07) \times 10^{-2}$
<i>B. infantis</i>		
AX	xylose	-
	arabinose	$(1.13 \pm 0.16) \times 10^{-3}$
Glc	xylose	-
	arabinose	$(1.64 \pm 0.40) \times 10^{-3}$

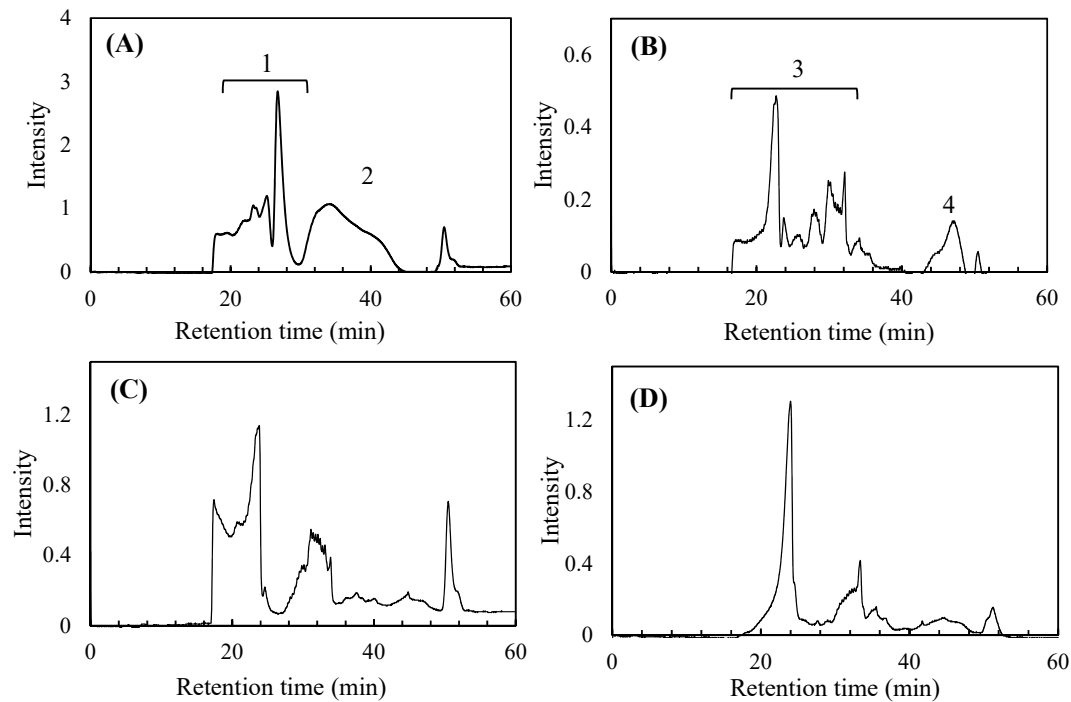
*Note:* Detection threshold of arabinose and xylose was  $\sim 1 \times 10^{-3}$  g/L.

### 3.4 Carbohydrate profiles in *B. longum* culture

Figure 2 shows the GPC (MW) profiles of *B. longum* culture medium containing AX or glucose as the carbon source. As shown in Table S1, the MW of AX was  $3.6 \times 10^5$  Da. In

Figure 2A, the peak around 38 min should indicate AX before bacterial fermentation which was overlapped with a broad and large peak 2 around 34.08 min. The multiple peaks (peak group 1) appearing between 17.4 and 29.7 min were probably attributed to the ingredients of culture medium. After bacterial fermentation (Figure 2B), the areas of group peak 1 and 2 were all decreased and multiple peaks appeared between 16.5 and 40 min (peak group 3). The peak around 38 min in Figure 2A disappeared, due probably to the consumption of AX and some other nutrients in the medium by *B. longum*. A new peak 4 at 47.42 min (~2700 Da) appeared in Figure 2B with the AX medium but not with the glucose medium at the same retention time (Figure 2C & D), which was probably derived from the hydrolysis of AX or metabolic products by the *B. longum* cells during AX fermentation.

Figure S2 shows the chromatograms of monosaccharides in the culture medium and the cell extract after *B. longum* fermentation on AX. No xylose or arabinose was detected in the culture medium (Figure S2A), implying that no enzymes were secreted out of the cells to hydrolyse AX into the constituent monosaccharides. This was consistent with the finding from the enzyme activity analysis (Table 3) that  $\alpha$ -L-arabinosidase or  $\beta$ -xylosidase was not detected in the culture medium. No xylose or arabinose was detected in the cell extract (Figure S2B), which had probably been completely consumed during the bacterial fermentation.



406 Figure 2 GPC profiles of the culture medium containing arabinoxylan (A, B) or glucose (C, D)  
407 before (A, C) and after (B, D) fermentation (24 h) by *B. longum* (Peak group 1, culture medium  
408 ingredients; Peak 2, AX overlapped with medium ingredients; Peak group 3, remaining  
409 medium ingredients; Peak 4, AX residues or bacterial metabolites).

410

411 Table 5 Monosaccharide composition and concentration of AX in cell extract and culture  
412 medium before and after *B. longum* fermentation.

Location	Fermentation	Monosaccharide	Conc. (g/L)
Culture medium	Before	xylose	3.38 ± 0.22
		arabinose	1.68 ± 0.13
	After	xylose	0.60 ± 0.02
		arabinose	0.17 ± 0.01
Cell extract	Before	xylose	-
		arabinose	-
	After	xylose	0.04 ± 0.004
		arabinose	0.02 ± 0.001

The native AX used in this study was composed of xylose and arabinose at a mole ratio of 2.0:1 (Table 5) and the concentration of AX was the sum of xylose and arabinose (5.06 g/L). After bacterial fermentation, the concentrations of xylose and arabinose in the culture medium decreased sharply, suggesting that both the backbone and branches of AX were consumed by *B. longum*. The mole ratio of xylose to arabinose after fermentation was increased to 3.5:1, suggesting the preference for the side chains by this bacterial strain. Although there was no detectable free xylose or arabinose in the cell extract cultured on native AX (Figure S2B), small amounts of xylose and arabinose were detected after acid hydrolysis of AX. This confirmed that the hydrolysed AX or AXOS could be transported directly into the bacterial cell and both the backbone and side chains were hydrolysed into monosaccharides intracellularly, and consumed immediately by the bacteria.

### 3.5 Influence of AX side chains on bacterial growth

The change in the side chains of AX during *B. longum* culture was detected by <sup>1</sup>H NMR (Figure 3) and the signals were assigned according to Hoffmann et al (1992) and Littuen et al (2015). At 0 h, the first broad peak around 5.3 ppm was the overlap of two peaks, one attributed to the ingredients of medium and the other (peak 1, 5.29 ppm) to the arabinose mono-substitution at the C3 position. The bacteria started to consume AX after 8 h of incubation. At 12 h, peak 1 disappeared completely while peak 2 (5.17 ppm) and peak 3 (5.12 ppm) both representing the di-substitution still had some signals and 4 hours later, AX was nearly exhausted. The higher utilization rate of peak 1 indicated that *B. longum* preferred the single-branch regions. This could also be confirmed by the bacterial growth (Figure 4C), attaining the

highest OD value in the culture medium containing single-substituted AX (AX-S), followed by AX, glucose, and then double-substituted AX (AX-D). The gradual disappearing of xylose residues (Figure 3, peak 4, 4.38 ppm) during fermentation further confirmed the degradation and consumption of AX backbones by the bacteria. Signals at 5.1 and 5.31 ppm probably arose from soluble starch in RCM medium (Tizzotti et al., 2011). These three peaks existed even when there was no glucose or AX in the medium, suggesting that they were originated from the RCM medium. Figure 3 also showed that these signals maintained their intensities even after bacterial fermentation. In general, soluble starch at a low concentration (1 g/L) in RCM medium is used to detoxify metabolic by-products and usually not consumed by the bacteria.

The preference for the specific structure regions of the AX polymer chain by the bifidobacteria as well as the growth rates of *B. longum* on different carbon sources (Figure 1B) strongly suggested that a specific chain structure of AX containing side chains was recognized by the bacterial cell to initiate the uptake and metabolism process of AX. Double substitution in the AX chain could cause obstruction of the specific structures to be recognized by the bacterial cell. Moderate acid hydrolysis of AX for short period of time probably removed the obstruction, facilitating the utilization by the bacterial cell to a higher growth rate (e.g. with AX-10). However, prolonged acid hydrolysis of AX led to a dramatic destruction of the structures and the resulting hydrolysate could not be recognized, and well utilized by the bacterial cell for growth (e.g. with AX-60). Therefore, the utilization rate as well as the growth rate in the bacterial cultures was much higher with AX-10 and AX-S than AX, AX-30, AX-60 and AX-D.



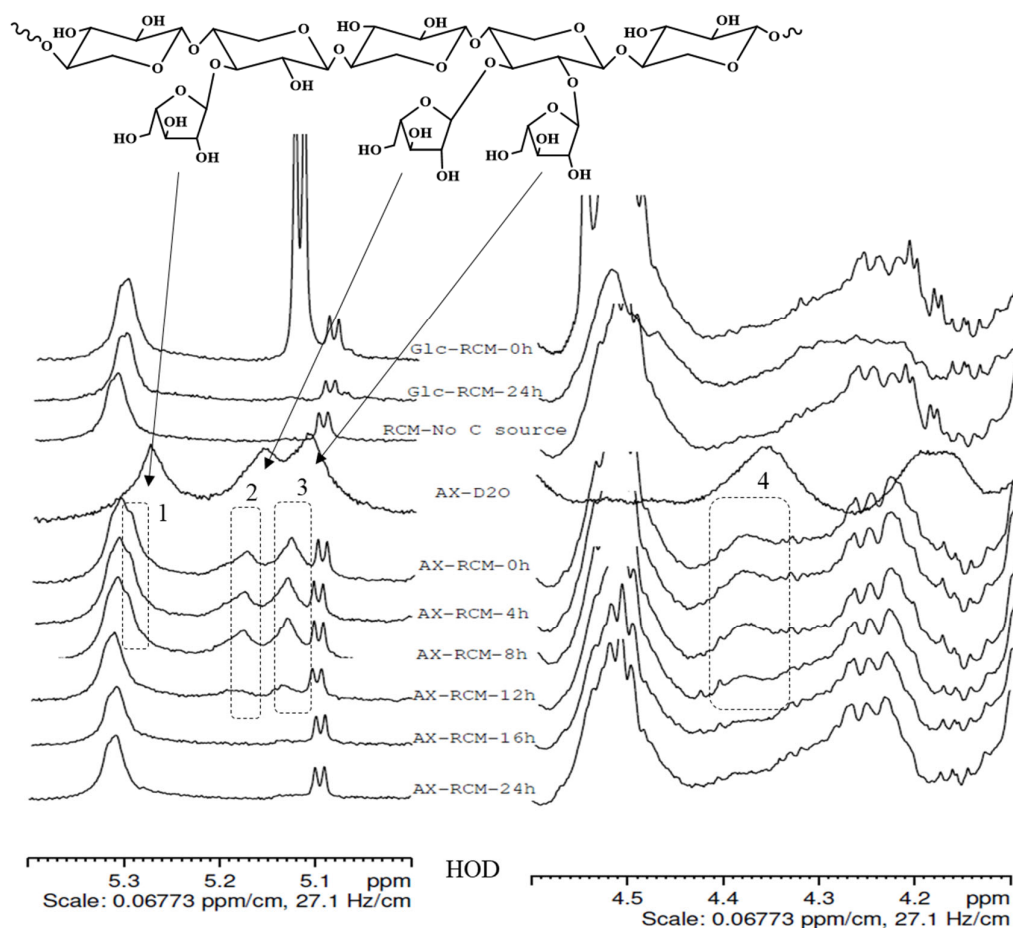


Figure 3  $^1\text{H}$  NMR spectra of culture medium containing AX during 24-hour culture of *B. longum*. The chemical shifts of arabinofuranosyl mono-substitution at C3, mono-substitution at C2 or di-substitution at C3, and di-substitution at C2 were 5.29, 5.17 and 5.12 ppm, respectively, and xylopyranosyl residues were at 4.38 ppm.

According to the sidechain linkage analysis of AX-S and AX-D (Figure 4A & B) and the bacterial growth (Figure 4C), *B. longum* could utilize the side chain in AX-S with both 1,2- and 1,3-L-arabinofuranosyl linkage. Similarly, a recent study has shown that an intracellular  $\alpha$ -L-arabinofuranosidase extracted from *B. longum* had the ability to cleave 1,2- and 1,3-L-arabinofuranosyl linkage on the side chains of both AX and arabinan (Komeno, Hayamizu, Fujita, & Ashida, 2019). This indicates that the spatial structure of the side chain on AX rather

than its linkage was the key factor for its utilization by *B. longum*. This also provides another piece of evidence that *B. longum* hydrolysed the side chains of AX intracellularly.

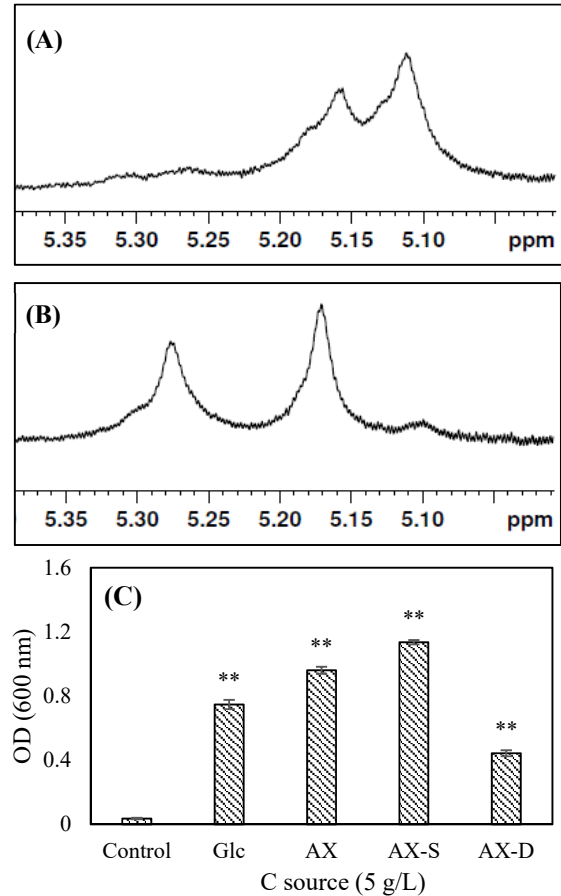


Figure 4 <sup>1</sup>H NMR of (A) double substituted arabinoxylan (AX-D) and (B) single substituted arabinoxylan (AX-S). (C) Growth of *B. longum* on different carbon (C) sources (\*\*:  $P < 0.01$  by  $t$  - test).

### 3.6 Genomic analysis of AX metabolism enzymes

The genome size of *B. longum* is 2,382,692 bp and the genome contained 60.3% of guanine and cytosine (G + C) which was within the typical range of *Actinobacteria* (Ventura et al., 2007), and 2058 probable coding regions were identified comprising 85% of the genome.

480 There were 78 noncoding RNA genes including 76 tRNA and 2 rRNA. Of the coding regions,  
 481 1569 (76%) were annotated to COG family (Figure S3), among which 383 (24%) were assigned  
 482 to function unknown (Figure S4). Of those unknown genes, 129 were identified according to  
 483 homologs from other bacterial strains and the remaining 254 genes were either specific to *B.*  
 484 *longum* or unidentified in other strains. More than 10.7% of the total predicted proteins were  
 485 assigned to carbohydrate transport and metabolism (G group) in COG family, which was 45%  
 486 more than *Lactobacillus lactis*, *B. halodurans* and *B. subtilis*, 27% more than *B. bifidum*, and  
 487 22% more than *B. longum* NCC 2705 (Schell et al., 2002; Turrone et al., 2010). This suggests  
 488 the strong ability of *B. longum* to utilize various non-digestible carbohydrates, which is  
 489 important for its adaptation to the lower human GIT. However, some other species like *B.*  
 490 *infantis* had the similar content of predicted proteins assigned to G group in COG annotation  
 491 (Sela et al., 2008). This was due to the capability of *B. infantis* for utilization of human milk  
 492 oligosaccharides. Therefore, a *B. infantis* strain was also analysed of its enzyme activity for  
 493 comparison in the present study (Tables 3&4). Some bacterial strains incapable of utilizing AX  
 494 might be able to metabolise other carbon sources, to generate a very high content of predicted  
 495 proteins responsible for carbohydrate transport and metabolism. Several ATP-binding cassette  
 496 (ABC)-type transporters involved in membrane transport of arabinose, xylose and  
 497 xylooligosaccharide were found in *B. longum* (Figure S5), confirming the results in Figure 1B  
 498 that this strain could grow on these carbon sources even though the utilization was less efficient  
 499 than AX. According to CAZy database, there were 81 predicted proteins annotated to  
 500 carbohydrate active enzymes (Figure S6), 62% of which belongs to glycoside hydrolases  
 501 including 3  $\alpha$ -L-arabinofuranosidase, 3 xylanase and 1 arabinosidase (Table S1). However,

there was no  $\beta$ -xylosidase annotated in this strain. Results in Table 3 and 4 show that the activity of  $\beta$ -xylosidase was detected intracellularly. Therefore, a novel  $\beta$ -xylosidase or a dual-specific enzyme should exist in this strain to hydrolyse the non-reducing end of AX backbone and is yet to be identified.

### **3.7 Metabolism of AX by *B. longum***

It has been suggested that the ABC-transporter system is employed by bifidobacteria for transportation of multiple carbohydrates including oligosaccharides and polysaccharides through the bacterial cell membrane (Koropatkin, Cameron, & Martens, 2012). Therefore, a model based on the ABC transporter system was proposed to describe the possible strategy for uptake and metabolism of AX and its hydrolysates in the *B. longum* cell based on the findings from this study (Figure 5). According to this model, the large AX molecule was partially hydrolysed by free endo-xylanase (or together with a cell-wall endo-xylanase) in the culture medium to relatively large oligosaccharides. A specific structure involving the side chains of AXOS was then recognized by the solute binding protein on the cell surface and transported directly into the cell by ABC transporters. AXOS in the bacterial cell was further hydrolysed by endo-xylanase into smaller oligosaccharides.  $\alpha$ -L-arabinosidase and  $\beta$ -xylosidase or a dual-specific enzyme acted synergistically to release monosaccharides.

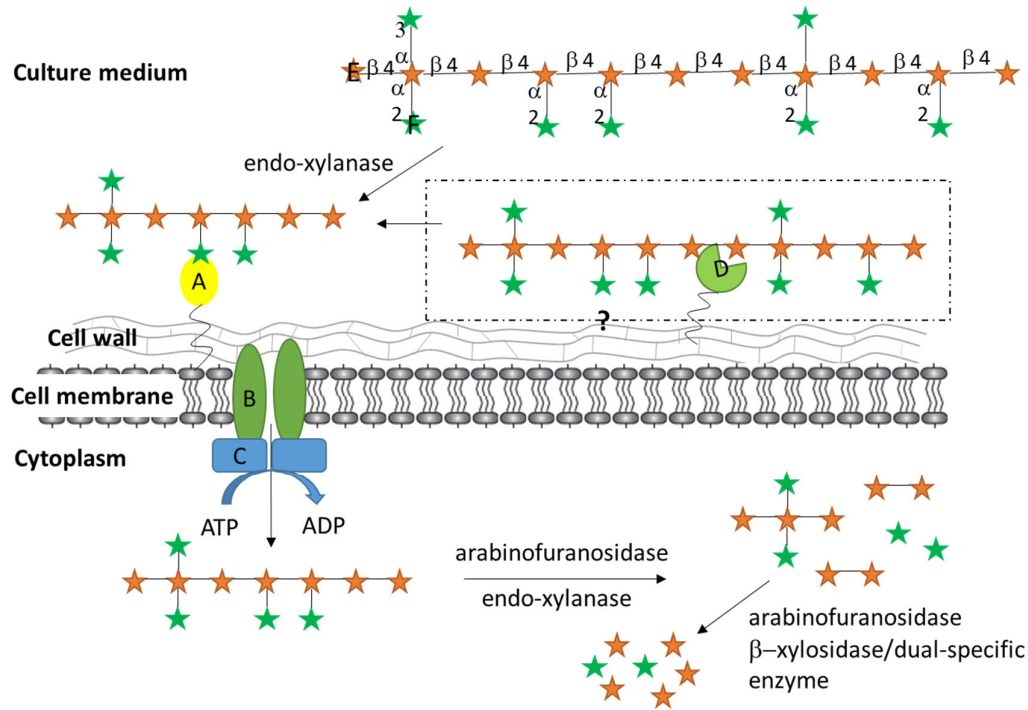


Figure 5 Strategies of arabinoxylan metabolism by *B. longum*. (A) solute binding protein, (B) membrane permease subunit, (C) ATPase, (D) cell wall endo-xylanase, (E) xylose and (F) arabinose.

In contrast, a few previous studies on the metabolism of AX, AXOS and XOS by bifidobacteria have suggested that the cleavage of arabinose substituents by *B. longum* occurred extracellularly, and the free arabinose and short fractions of XOS but not long chain of xylose could be metabolised by some of *B. longum* strains (Crittenden et al., 2002; Feng et al., 2018; Rivière et al., 2014). However, the present study suggested that arabinose was hydrolysed inside the cell, and long chain AX was preferred by *B. longum* while XOS and arabinose were less efficiently utilized. This can be explained by the different characteristics of various *B. longum* strains and the capability of bifidobacteria for degrading AX and AXOS is strain-dependent. On the other hand, Feng et al. (2018) have suggested that there exist endo-xylanases

on the gut microbial cell surface. Since the cell-wall xylanase was not determined in the present study, its involvement in the AX degradation by *B. longum* remains to be confirmed.

#### 4. Conclusions

This study provided a molecular and mechanistic model for the uptake and degradation of AX by the cell of a *B. longum* strain. Both the backbone and side chains in AX could be utilized by this strain. The degradation of xylose backbones occurred both outside and inside the bacterial cell while the cleavage of arabinose substitutions was intracellular. The fine structure of AX played an important role in governing its fermentation efficiency. Native and partially hydrolysed AX with a higher degree of polymerization and a high side chain content were more preferable for utilization by *B. longum* for growth. The *B. longum* strain grew more favourably on single-substituted than double-substituted AX fractions. The genomic analysis results did not show the presence of  $\beta$ -xylosidase in *B. longum*. A novel or a dual-specific enzyme remains to be discovered in this bacterium. In addition, further studies should be performed to reveal the membrane recognition and transportation mechanisms of AX by the bacterial cell. It is also worthwhile to identify the enzymes which are specifically responsible for both extracellular and intracellular degradation of AX and its lower MW fractions.

#### Acknowledgments

This work was supported by the Hong Kong Polytechnic University and the Research Grant Council of the Hong Kong SAR Government through RGC General Research Fund (PolyU 152707/16E).

## References

- Chassard, C., Goumy, V., Leclerc, M., Del'homme, C., & Bernalier-Donadille, A. (2007). Characterization of the xylan-degrading microbial community from human faeces. *FEMS microbiology ecology*, 61(1), 121-131.
- Chen, X., Siu, K.-C., Cheung, Y.-C., & Wu, J.-Y. (2014). Structure and properties of a (1→3)-β-d-glucan from ultrasound-degraded exopolysaccharides of a medicinal fungus. *Carbohydrate polymers*, 106, 270-275.
- Crittenden, R., Karppinen, S., Ojanen, S., Tenkanen, M., Fagerström, R., Mättö, J., Poutanen, K. (2002). In vitro fermentation of cereal dietary fibre carbohydrates by probiotic and intestinal bacteria. *Journal of the Science of Food and Agriculture*, 82(8), 781-789.
- Derensy-Dron, D., Krzewinski, F., Brassart, C., & Bouquelet, S. (1999). β-1, 3-Galactosyl-N-acetylhexosamine phosphorylase from *Bifidobacterium bifidum* DSM 20082: characterization, partial purification and relation to mucin degradation. *Biotechnology and applied biochemistry*, 29(1), 3-10.
- Eckburg, P. B., Bik, E. M., Bernstein, C. N., Purdom, E., Dethlefsen, L., Sargent, M., Relman, D. A. (2005). Diversity of the human intestinal microbial flora. *Science*, 308(5728), 1635-1638.
- Falony, G., Vlachou, A., Verbrugghe, K., & Vuyst, L. D. (2006). Cross-Feeding between *Bifidobacterium longum* BB536 and Acetate-Converting, Butyrate-Producing Colon Bacteria during Growth on Oligofructose. *Applied and environmental microbiology*, 72(12), 7835-7841.
- Favier, C. F., Vaughan, E. E., De Vos, W. M., & Akkermans, A. D. (2002). Molecular monitoring of succession of bacterial communities in human neonates. *Appl. Environ. Microbiol.*, 68(1), 219-226.
- Feng, G., Flanagan, B. M., Mikkelsen, D., Williams, B. A., Yu, W., Gilbert, R. G., & Gidley, M. J. (2018). Mechanisms of utilisation of arabinoxylans by a porcine faecal inoculum: competition and co-operation. *Scientific reports*, 8(1), 4546.
- Geraylou, Z., Souffreau, C., Rurangwa, E., D'hondt, S., Callewaert, L., Courtin, C. M., . . . Ollevier, F. (2012). Effects of arabinoxylan-oligosaccharides (AXOS) on juvenile Siberian

sturgeon (*Acipenser baerii*) performance, immune responses and gastrointestinal microbial community. *Fish & shellfish immunology*, 33(4), 718-724.

Hoffmann, R. A., Geijtenbeek, T., Kamerling, J. P., & Vliegthart, J. F. (1992). <sup>1</sup>H-Nmr study of enzymically generated wheat-endosperm arabinoxylan oligosaccharides: structures of hepta-to tetradeca-saccharides containing two or three branched xylose residues. *Carbohydrate research*, 223, 19-44.

Hopkins, M. J., Englyst, H. N., Macfarlane, S., Furrie, E., Macfarlane, G. T., & McBain, A. J. (2003). Degradation of cross-linked and non-cross-linked arabinoxylans by the intestinal microbiota in children. *Applied & Environmental Microbiology*, 69(11), 6354-6360.

Izydorczyk, M. S., & Biliaderis, C. G. (1995). Cereal arabinoxylans: advances in structure and physicochemical properties. *Carbohydrate polymers*, 28(1), 33-48.

Jaskari, J., Kontula, P., Siitonen, A., Jousimies-Somer, H., Mattila-Sandholm, T., & Poutanen, K. (1998). Oat  $\beta$ -glucan and xylan hydrolysates as selective substrates for *Bifidobacterium* and *Lactobacillus* strains. *Applied microbiology and biotechnology*, 49(2), 175-181.

Komeno, M., Hayamizu, H., Fujita, K., & Ashida, H. (2019). Two Novel  $\alpha$ -L-Arabinofuranosidases from *Bifidobacterium longum* subsp. *longum* Belonging to Glycoside Hydrolase Family 43 Cooperatively Degrade Arabinan. *Applied & Environmental Microbiology*, 85(6), e02582-02518.

Kondepudi, K. K., Ambalam, P., Nilsson, I., Wadström, T., & Ljungh, Å. (2012). Prebiotic-non-digestible oligosaccharides preference of probiotic bifidobacteria and antimicrobial activity against *Clostridium difficile*. *Anaerobe*, 18(5), 489-497.

Koropatkin, N. M., Cameron, E. A., & Martens, E. C. (2012). How glycan metabolism shapes the human gut microbiota. *Nature Reviews Microbiology*, 10(5), 323.

Lagaert, S., Pollet, A., Delcour, J. A., Lavigne, R., Courtin, C. M., & Volckaert, G. (2011). Characterization of two  $\beta$ -xylosidases from *Bifidobacterium adolescentis* and their contribution to the hydrolysis of prebiotic xylooligosaccharides. *Applied Microbiology and Biotechnology*, 92(6), 1179-1185.

Lagier, J. C., Khelaihia, S., Alou, M. T., et al. (2016). Culture of previously uncultured members of the human gut microbiota by culturomics. *Nature Microbiology*, 7(1), 16203.



616 Leth, M. L., Ejby, M., Workman, C., Ewald, D. A., Pedersen, S. S., Sternberg, C., Westereng,  
617 B. (2018). Differential bacterial capture and transport preferences facilitate co-growth on  
618 dietary xylan in the human gut. *Nature microbiology*, 3(5), 570-580.

619 Mendis, M., Leclerc, E., & Simsek, S. (2016). Arabinoxylans, gut microbiota and immunity.  
620 *Carbohydrate polymers*, 139, 159-166.

621 Michlmayr, H., Hell, J., Lorenz, C., Böhmendorfer, S., Rosenau, T., & Kneifel, W. (2013).  
622 Arabinoxylan-Oligosaccharide Hydrolysis by Family 43 and 51 Glycosidases from  
623 *Lactobacillus brevis* DSM 20054. *Applied and environmental microbiology*, AEM. 02130-  
624 02113.

625 Mori, M., Eda, S., & Katô, K. (1979). Two Xyloglucan Oligosaccharides Obtained by  
626 Cellulase-degradation, of Tobacco Arabinoxylglucan. *Agricultural and Biological*  
627 *Chemistry*, 43(1), 145-149.

628 Neyrinck, A. M., Possemiers, S., Druart, C., Van de Wiele, T., De Backer, F., Cani, P. D., . . .  
629 Delzenne, N. M. (2011). Prebiotic effects of wheat arabinoxylan related to the increase in  
630 bifidobacteria, Roseburia and Bacteroides/Prevotella in diet-induced obese mice. *PloS one*,  
631 6(6), e20944-e20944.

632 Pastell, H., Westermann, P., Meyer, A. S., Tuomainen, P., & Tenkanen, M. (2009). In vitro  
633 fermentation of arabinoxylan-derived carbohydrates by bifidobacteria and mixed fecal  
634 microbiota. *Journal of Agricultural and Food Chemistry*, 57(18), 8598-8606.

635 Pokusaeva, K., Fitzgerald, G. F., & van Sinderen, D. (2011). Carbohydrate metabolism in  
636 *Bifidobacteria*. *Genes & nutrition*, 6(3), 285.

637 Rastall, R. A., Gibson, G. R., Gill, H. S., Guarner, F., Klaenhammer, T. R., Pot, B., . . . Sanders,  
638 M. E. (2005). Modulation of the microbial ecology of the human colon by probiotics,  
639 prebiotics and synbiotics to enhance human health: an overview of enabling science and  
640 potential applications. *FEMS microbiology ecology*, 52(2), 145-152.

641 Rivière, A., Moens, F., Selak, M., Maes, D., Weckx, S., & De Vuyst, L. (2014). The ability of  
642 bifidobacteria to degrade arabinoxylan oligosaccharide constituents and derived  
643 oligosaccharides is strain dependent. *Applied and environmental microbiology*, 80(1), 204-  
644 217.

645 Rose, D. J., Patterson, J. A., & Hamaker, B. R. (2009). *Structural Differences among Alkali-*  
646 *Soluble Arabinoxylans from Maize (Zea mays), Rice (Oryza sativa), and Wheat (Triticum*  
647 *aestivum) Brans Influence Human Fecal Fermentation Profiles* (Vol. 58).

648 Rycroft, C., Jones, M., Gibson, G. R., & Rastall, R. (2001). A comparative in vitro evaluation  
649 of the fermentation properties of prebiotic oligosaccharides. *Journal of applied*  
650 *microbiology*, 91(5), 878-887.

651 Schell, M. A., Karmirantzou, M., Snel, B., Vilanova, D., Berger, B., Pessi, G., Delley, M.  
652 (2002). The genome sequence of Bifidobacterium longum reflects its adaptation to the  
653 human gastrointestinal tract. *Proceedings of the National Academy of Sciences*, 99(22),  
654 14422-14427.

655 Sela, D., Chapman, J., Adeuya, A., Kim, J., Chen, F., Whitehead, T., German, J. (2008). The  
656 genome sequence of Bifidobacterium longum subsp. infantis reveals adaptations for milk  
657 utilization within the infant microbiome. *Proceedings of the National Academy of Sciences*,  
658 105(48), 18964-18969.

659 Song, A.-X., Mao, Y.-H., Siu, K.-C., & Wu, J.-Y. (2018). Bifidogenic effects of Cordyceps  
660 sinensis fungal exopolysaccharide and konjac glucomannan after ultrasound and acid  
661 degradation. *International journal of biological macromolecules*, 111, 587-594.

662 Tap, J., Mondot, S., Levenez, F., Pelletier, E., Caron, C., Furet, J. P., Nalin, R. (2009). Towards  
663 the human intestinal microbiota phylogenetic core. *Environmental microbiology*, 11(10),  
664 2574-2584.

665 Tizzotti, M. J., Sweedman, M. C., Tang, D., Schaefer, C., & Gilbert, R. G. (2011). New 1H  
666 NMR procedure for the characterization of native and modified food-grade starches. *Journal*  
667 *of Agricultural and Food Chemistry*, 59(13), 6913-6919.

668 Turroni, F., Bottacini, F., Foroni, E., Mulder, I., Kim, J.-H., Zomer, A., Giubellini, V. (2010).  
669 Genome analysis of Bifidobacterium bifidum PRL2010 reveals metabolic pathways for  
670 host-derived glycan foraging. *Proceedings of the National Academy of Sciences*, 107(45),  
671 19514-19519.

672 Van den Abbeele, P., Gérard, P., Rabot, S., Bruneau, A., El Aidy, S., Derrien, M. & Verstraete,  
673 W. (2011). Arabinoxylans and inulin differentially modulate the mucosal and luminal gut

674 microbiota and mucin-degradation in humanized rats. *Environmental microbiology*, 13(10),  
675 2667-2680.

676 van den Broek, L. A., Hinz, S. W., Beldman, G., Vincken, J. P., & Voragen, A. G. (2008).  
677 Bifidobacterium carbohydrases - their role in breakdown and synthesis of (potential)  
678 prebiotics. *Molecular nutrition & food research*, 52(1), 146-163.

679 Van Laere, K. M. J., Hartemink, R., Bosveld, M., Schols, H. A., & Voragen, A. G. J. (2000).  
680 Fermentation of plant cell wall derived polysaccharides and their corresponding  
681 oligosaccharides by intestinal bacteria. *Journal of Agricultural and Food Chemistry*, 48(5),  
682 1644-1652.

683 Van Laere, K. M. J., Voragen, C., Kroef, T., Van den Broek, L., Beldman, G., & Voragen, A.  
684 (1999). Purification and mode of action of two different arabinoxylan  
685 arabinofuranohydrolases from Bifidobacterium adolescentis DSM 20083. *Applied*  
686 *microbiology and biotechnology*, 51(5), 606-613.

687 Vardakou, M., Palop, C. N., Gasson, M., Narbad, A., & Christakopoulos, P. (2007). In vitro  
688 three-stage continuous fermentation of wheat arabinoxylan fractions and induction of  
689 hydrolase activity by the gut microflora. *International journal of biological macromolecules*,  
690 41(5), 584-589.

691 Ventura, M., Canchaya, C., Tauch, A., Chandra, G., Fitzgerald, G. F., Chater, K. F., & van  
692 Sinderen, D. (2007). Genomics of Actinobacteria: tracing the evolutionary history of an  
693 ancient phylum. *Microbiology and molecular biology reviews : MMBR*, 71(3), 495-548.

694 Wang, H.-x., Zhao, J., Li, D.-m., Song, S., Song, L., Fu, Y.-h., & Zhang, L.-p. (2015).  
695 Structural investigation of a uronic acid-containing polysaccharide from abalone by graded  
696 acid hydrolysis followed by PMP-HPLC-MSn and NMR analysis. *Carbohydrate research*,  
697 402, 95-101.

698 Zeng, H., Xue, Y., Peng, T., & Shao, W. (2007). Properties of xylanolytic enzyme system in  
699 bifidobacteria and their effects on the utilization of xylooligosaccharides. *Food chemistry*,  
700 101(3), 1172-1177.